AIP | Applied Physics Letters

Perpendicular anisotropy L10-FePt based pseudo spin valve with Ag spacer layer

P. Ho, G. C. Han, R. F. L. Evans, R. W. Chantrell, G. M. Chow et al.

Citation: Appl. Phys. Lett. **98**, 132501 (2011); doi: 10.1063/1.3571450
View online: http://dx.doi.org/10.1063/1.3571450
View Table of Contents: http://apl.aip.org/resource/1/APPLAB/v98/i13
Published by the American Institute of Physics.

Perpendicular anisotropy $L1_0$-FePt based pseudo spin valve with Ag spacer layer

P. Ho,[1,2] G. C. Han,[2] R. F. L. Evans,[3] R. W. Chantrell,[3] G. M. Chow,[1] and J. S. Chen[1,a)]
[1]*Department of Materials Science and Engineering, National University of Singapore, Singapore 117576*
[2]*Data Storage Institute, Agency of Science, Technology and Research (A*STAR), Singapore 117608*
[3]*Department of Physics, University of York, York YO10 5DD, United Kingdom*

(Received 11 January 2011; accepted 3 March 2011; published online 28 March 2011)

The effects of post-annealing temperature of the Ag spacer layer on the structural, magnetic, spin, and magneto-transport properties of perpendicular anisotropy pseudo spin valves $L1_0$-$Fe_{50}Pt_{50}$/Ag/$L1_0$-$Fe_{50}Pt_{50}$ had been investigated. The Ag spacer layer was post-annealed at various temperatures of 300, 400, and 500 °C. A giant magnetoresistance ratio of 1.1% and 2.2% was achieved at room temperature and 77 K, respectively, when Ag was post-annealed at 300 °C. This was a significant improvement from the use of Au, Pt, and Pd spacer materials. © *2011 American Institute of Physics*. [doi:10.1063/1.3571450]

Spin valve systems with perpendicular magnetization have become more attractive as they allow a reduction in critical spin transfer current and shrinkage of spintronics devices, while ensuring thermal stability with the use of high magnetocrystalline anisotropy (K_u) materials.[1] $L1_0$-FePt is a potential candidate due to its high K_u of 7×10^7 erg/cm^3 and has been used in spin valves with Au, Pt, and Pd spacer layers. The use of Au and Pt spacer yielded low giant magnetoresistance (GMR) values of 0.08% and 0.65%, respectively, due to the high tendency for these heavy elements to depolarize electron spins through high spin orbit scattering. The use of a lighter noble element Pd improved the GMR to 0.80%.[2,3] Here, Ag is considered a suitable candidate for the spacer as it is a noble metal with atomic number (47) close to that of Pd (46). Earlier studies have also shown that Ag (001) can induce well-oriented epitaxial $L1_0$-FePt (001) texture at a lower ordering temperature.[4,5] The quality of the $L1_0$-FePt/Ag interface affects the scattering of the conduction electrons and ultimately, the GMR. Post-annealing treatment after film deposition alters the interfacial properties at the spacer/ferromagnet interface.[6,7] In this letter, the effects of post-annealing temperature of the Ag spacer on the structural, magnetic, spin, and magneto-transport properties of the $L1_0$-FePt based pseudo spin valves (PSVs) were investigated.

Samples with the structure MgO substrate/$L1_0$-$Fe_{50}Pt_{50}$ (20 nm)/Ag (2.5 nm)/$L1_0$-$Fe_{50}Pt_{50}$ (5 nm) were prepared using magnetron sputtering system with a base pressure better than 3×10^{-7} Torr. Bottom and top FePt layers were deposited at 450 °C and 300 °C, respectively. The Ag spacer was deposited at 150 °C and subsequently post-annealed at 300, 400, or 500 °C. Crystallographic structures were studied using x-ray diffraction. Surface roughness was probed using the atomic force microscope. Transmission electron microscopy (TEM) was carried out to study the microstructure. Magnetic properties were characterized by the vibrating sample magnetometer. Current-in-plane (CIP) resistance measurements were made using a four point probe in the presence of a perpendicular-to-plane field.

Table I summarizes the root-mean-square roughness of the Ag spacer with various post-annealing temperatures. With increasing post-annealing temperature from 300 to 500 °C, the roughness of the Ag layer decreased by a factor of 2. TEM images (Fig. 1) show that with increasing Ag post-annealing temperature from 300 to 500 °C, the thickness of the spacer decreased from 2.2 to 1.4 nm although this was intended to be constant across all samples. At higher post-annealing temperatures, a greater extent of interdiffusion between bottom $L1_0$-FePt and Ag occurred, causing a reduction in the Ag layer thickness.

Figure 2 shows the reciprocal space maps (RSMs) of the PSVs. The RSMs revealed intensity contour plots with a strong pronounced (002) MgO reflection, followed by a FePt reflection halo. Ag reflection was not observed. This was not an indication of poor Ag (002) texture but a result of the thin Ag film being unable to produce significant x-ray reflection relative to the background noise. This was supported by the observation of lattice fringes in the Ag spacer [Fig. 1(a) and inset of Fig. 1(b)], indicating the growth of (001) textured crystalline Ag film with Ag post-annealed at 300 and

TABLE I. Magnetic properties and characteristics of the PSVs with Ag post-annealed at (a) 300 °C, (b) 400 °C, and (c) 500 °C. δ is the estimated domain wall width where $\delta=\pi\sqrt{A/K_u}$, with $A=10^{-6}$ erg cm^{-1}.

Ag post-annealing temperature (°C)	Hard layer K_u ($\times10^7$ erg cm^{-3})	M_s (emu cm^{-3})	Hard layer coercivity (kOe)	Soft layer coercivity (kOe)	Ag roughness (nm)	δ (nm)
300	1.44	794	3.86	1.94	1.1	8.28
400	1.40	747	3.74	1.99	0.7	8.40
500	1.45	799	3.50	···	0.6	8.25

a)Author to whom correspondence should be addressed. Electronic mail: msecj@nus.edu.sg.

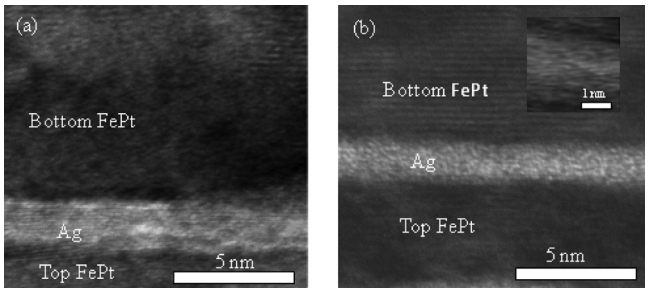

FIG. 1. TEM images of PSVs with Ag post-annealed at (a) 300 °C and (b) 500 °C. The inset shows the higher magnification TEM image of the PSV with Ag postannealed at 500 °C.

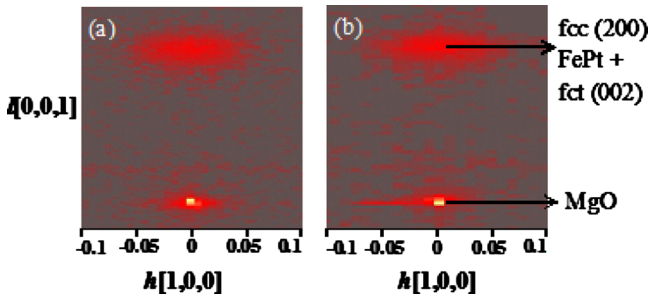

FIG. 2. (Color online) RSMs of the specular (002) reflections of MgO, Ag, and FePt when the Ag spacer was post-annealed at (a) 300 and (b) 500 °C. MgO (002) substrate is assigned to be the reference layer.

500 °C. The intensity contour plot of FePt is a representation of both fcc (200) and fct (002) since the difference in their lattice parameters is negligible. There were no major differences in the size of the FePt reflection halo among the RSMs, suggesting that the formation of $L1_0$-FePt (001) texture was not significantly affected by the Ag post-annealing temperature.

The PSVs with Ag post-annealed at 300 and 400 °C were exchange decoupled and exhibited little difference in their magnetic properties [Fig. 3(a)]. The thicker bottom $L1_0$-FePt possessed a higher coercivity than the thinner top $L1_0$-FePt. Thus, the harder bottom $L1_0$-FePt behaved as the fixed layer while softer top $L1_0$-FePt the free layer. Further increase in the Ag post-annealing temperature to 500 °C resulted in the disappearance of the kink in the hysteresis loop. The extensive interdiffusion between bottom $L1_0$-FePt and Ag led to a thinner Ag spacer which could not bring about exchange decoupling between the top and bottom $L1_0$-FePt. Atomic scale simulation carried out on the PSVs with Ag post-annealed at 300 and 500 °C [Fig. 3(b)] indicated a good fit with experimental results, where an increased interlayer exchange coupling strength was caused by a thinner and more heavily diffused Ag spacer post-annealed at 500 °C. Detailed simulation results will be described elsewhere.[8]

The switching field distribution (SFD) curves of the PSVs with Ag post-annealed at 300 [Fig. 3(c)] and 400 °C show two distinct peaks, demonstrating independent magnetization reversal of the $L1_0$-FePt layers. The SFD of the bottom $L1_0$-FePt layer increased when Ag post-annealing temperature increased from 300 to 400 °C, indicative of reduced exchange coupling between the bottom FePt particles at higher post-annealing temperature. This was due to the formation of more decoupled grains within the bottom $L1_0$-FePt layer, a result of increased Ag diffusion to the $L1_0$-FePt grain boundaries. When the Ag post-annealing temperature increased to 500 °C, the formation of a more granular FePt phase was expected. However, the derivative of the hysteresis loop reflected a narrower SFD for the bottom $L1_0$-FePt layer due to exchange coupling with the top layer [Fig. 3(d)].[9]

Figures 4(a)–4(d) show the MR loops of the PSVs with Ag post-annealed at the various temperatures. GMR ratios of 1.1% and 2.2% at room temperature and 77 K, respectively, were obtained when Ag was post-annealed at 300 °C. This was higher than previous reports of room temperature CIP measurements of $L1_0$-FePt based spin valves with Pt and Pd spacers and two orders of magnitude higher than that with Au spacer obtained from current perpendicular to plane measurements at 77 K.[2,3] The GMR observed was attributed to the spin dependent scattering of electrons from the trilayer interfaces as well as the domain walls and granular system within the $L1_0$-FePt layers. When current passed through the trilayer, GMR arose from the asymmetric scattering probability of the spin up and spin down electrons. With high K_u, a narrow domain wall width δ in the range of 8.25 to 8.40 nm was expected of the bottom $L1_0$-FePt layer [Table I]. This allowed domain wall scattering by the randomly aligned

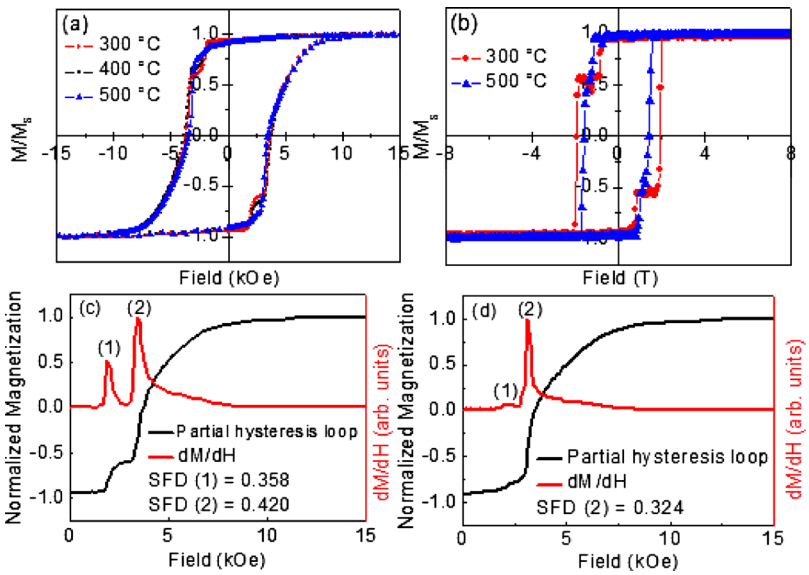

FIG. 3. (Color online) (a) Hysteresis loops of PSVs with varying Ag post-annealing temperatures of 300, 400, and 500 °C and (b) Simulated hysteresis loops of PSVs with Ag postannealing temperatures of 300 and 500 °C. Partial hysteresis loops and their derivatives, with SFD of the top and bottom $L1_0$-FePt layer labeled (1) and (2), respectively, for PSVs with Ag post-annealed at (c) 300 and (d) 500 °C.

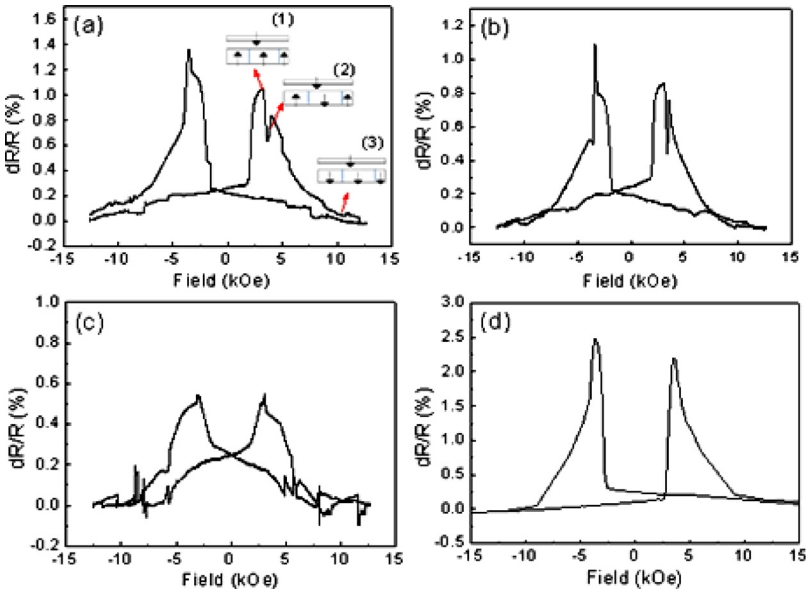

FIG. 4. (Color online) MR loops of PSVs for Ag post-annealed at (a) 300 °C, (b) 400 °C, and (c) 500 °C measured at room temperature and (d) Ag post-annealed at 300 °C measured at 77 K. The inset (a) indicates schematically the reversal behavior.

domains to contribute to GMR during magnetization reversal of the bottom $L1_0$-FePt layer, which occurred via domain nucleation and propagation.[10,11] An MR ratio of 0.2% due to domain wall scattering was previously reported in sputtered $L1_0$-FePt films.[11] In addition, high temperature post-annealing resulted in the formation of grains within the bottom $L1_0$-FePt layer. Hence, scattering of electrons at the interface of the FePt grains and non-magnetic Ag grain boundaries was also likely to have enhanced the GMR effect.[12,13]

With increasing Ag post-annealing temperature, the GMR ratio of the PSV decreased. Reduction in Ag spacer roughness by increasing the Ag post-annealing temperature had no effect in improving the GMR ratio. The decrease in GMR ratio at a Ag post-annealing temperature of 400 °C was due to a larger defect density in the bottom $L1_0$-FePt film with a higher degree of grain formation. The increased presence of grain boundaries reduced the electron mean free path and increased the spin independent scattering.[7] Further increase in the Ag post-annealing temperature to 500 °C resulted in a thinner spacer which could not decouple the $L1_0$-FePt layers. Scattering of the electrons at the interfaces of the trilayer ceased to contribute to the overall GMR with the $L1_0$-FePt layers perpetually assuming a low resistance parallel configuration. Instead, GMR was likely due to the combination of domain wall and granular scattering within the $L1_0$-FePt layers.

There was also a sharp observable discontinuity on both sides of the MR loop for Ag post-annealed at 300 and 400 °C. When the applied field was in the range between the soft and hard $L1_0$-FePt coercivity, anti-parallel magnetic configuration assumed by the $L1_0$-FePt layers resulted in the initial peak in the GMR ratio [inset 1 of Fig. 4(a)]. Beyond the hard layer coercivity, reversal of the hard $L1_0$-FePt layer magnetization began. Increasing formation of reversed domains within the hard layer with magnetization parallel to that of the soft layer led to a subsequent decline in the GMR ratio. However, the concurrent onset of the combined effects from domain wall and granular scatterings ultimately dominated and brought about the spike in GMR ratio [inset 2 of Fig. 4(a)].[14] At large applied fields, complete reversal of the bottom $L1_0$-FePt layer gave rise to a low resistance magnetic configuration [inset 3 of Fig. 4(a)]. It was further observed that the spike at each side of the MR loop was more distinct for Ag post-annealed at 400 °C. This was due to the greater extent of grain formation in the bottom $L1_0$-FePt, which increased the interfacial area present for granular scattering. In addition, the asymmetrical MR loops arose possibly due to the asymmetrical skew scattering of spin up and spin down electrons from spin orbit interaction.[15,16]

This work is partially supported by Agency of Science, Technology and Research (A*STAR), Singapore, SERC Grant No. 092-156-0118 and Ministry of Education, Singapore, Tier 1 funding Grant No. T11-1001-P04.

[1]J. G. Zhu, Proc. IEEE **96**, 1786 (2008).
[2]A. P. Mihai, J. P. Attané, L. Vila, C. Beigné, J. C. Pillet, and A. Marty, Appl. Phys. Lett. **94**, 122509 (2009).
[3]T. Seki, S. Mitani, K. Yakushiji, and K. Takanashi, Appl. Phys. Lett. **89**, 172504 (2006).
[4]Y. Hsu, S. Jeong, D. E. Laughlin, and D. N. Lambeth, J. Magn. Magn. Mater. **260**, 282 (2003).
[5]Z. L. Zhao, J. S. Chen, J. Ding, J. B. Yi, B. H. Liu, and J. P. Wang, Appl. Phys. Lett. **88**, 052503 (2006).
[6]A. Gupta, A. Paul, S. M. Chaudhari, and D. M. Phase, J. Phys. Soc. Jpn. **69**, 2182 (2000).
[7]E. M. Ho, A. K. Petford-Long, and A. Cerezo, J. Magn. Magn. Mater. **192**, 431 (1999).
[8]P. Ho, R. F. L. Evans, R. W. Chantrell, G. C. Han, G. M. Chow, and J. S. Chen, INTERMAG Conference Digest, Taipei, 25-29 April 2011 (http://intermag.onestep.com.tw/index.asp).
[9]T. Hauet, E. Dobisz, S. Florez, J. Park, B. Lengsfield, B. D. Terris, and O. Hellwig, Appl. Phys. Lett. **95**, 262504 (2009).
[10]S. Ishio, T. Yoshino, H. Saito, T. Suzuki, and K. Ohuchi, J. Magn. Magn. Mater. **239**, 217 (2002).
[11]K. M. Seemann, V. Baltz, M. Mackenzie, J. N. Chapman, B. J. Hickey, and C. H. Marrows, Phys. Rev. B **76**, 174435 (2007).
[12]A. Granovsky, F. Brouers, A. Kalitsov, and M. Chshiev, J. Magn. Magn. Mater. **166**, 193 (1997).
[13]S. J. Guilfoyle, R. J. Pollard, and P. J. Grundy, J. Phys. D: Appl. Phys. **29**, 29 (1996).
[14]A. P. Mihai, J. P. Attane, A. Marty, P. Warin, and Y. Samson, Phys. Rev. B **77**, 060401 (2008).
[15]O. Shaya, M. Karpovski, and A. Gerber, J. Appl. Phys. **102**, 043910 (2007).
[16]K. M. Seemann, Y. Mokrousov, A. Aziz, J. Miguel, F. Kronast, W. Kuch, M. G. Blamire, A. T. Hindmarch, B. J. Hickey, I. Souza, and C. H. Marrows, Phys. Rev. Lett. **104**, 076402 (2010).